Tropical Journal of Pharmaceutical Research April 2022; 21 (4): 733-739
ISSN: 1596-5996 (print); 1596-9827 (electronic)

Available online at http://www.tjpr.org
http://dx.doi.org/10.4314/tjpr.v21i4.8

Original Research Article

Effects of microRNA-129-5p on hepatic fibrosis and primary hepatic stellate cell proliferation and migration in rats

Chen Li[1], Yaohong Xu[1]*, Xiaofu Lin[2]
[1]Department of Liver Disease, [2]Department of Pharmacy, Lishui City People's Hospital, Lishui, Zhejiang 323000, China

For correspondence: **Email: xuyaohong0316@163.com; **Tel:** +86-578 -2780174*

Sent for review: 1 October 2021 *Revised accepted: 17 March 2022*

Abstract

Purpose: *To investigate the effects and mechanism of microRNA (miR)-129-5p in hepatic fibrosis and hepatic stellate cell proliferation and migration in rats.*
Methods: *Forty Sprague-Dawley rats were randomly divided into control and model groups. Carbon tetrachloride (CCl_4)-induced hepatic fibrosis was established in the model group. Hematoxylin and eosin staining was used to observe rat liver pathological sections. Sirius red staining was used to assess collagen deposition, while quantitative real-time polymerase chain reaction was used to evaluate miR-129-5p expression in the rat liver during hepatic fibrosis. Three groups of rat primary hepatic stellate cells (HSCs) (miR-129-5p overexpression group, negative control lentivirus group and blank control group) were prepared. Cell proliferation and migration were determined using Cell Counting Kit-8 and Transwell assay, respectively. Serum- and glucocorticoid-regulated kinase 3 (SGK3), β-catenin, and α-smooth muscle actin (α-SMA) expression were evaluated by Western blotting, while dual luciferase reporter gene assay was used to evaluate whether SGK3 is an miR-129-5p target.*
Results: *miR-129-5p expression was significantly reduced during the progression of CCl_4-induced rat hepatic fibrosis ($p < 0.05$). The proliferation rate and migration ability of the primary HSCs in the miR-129-5p mimics group were significantly lower than those in the miR-129-5p NC and blank control groups ($p < 0.05$). Protein expression of SGK3, β-catenin, and α-SMA in the miR-129-5p mimics group was reduced ($p < 0.05$), and miR-129-5p showed targeted binding to SGK3.*
Conclusion: *MiR-129-5p down-regulates the expression of β-catenin through targeted regulation of SGK3 to inhibit HSC activation, providing novel insight into design of a potential treatment strategy for hepatic fibrosis.*

Keywords: *MicroRNA-129-5p, SGK3, Hepatic stellate cells, Hepatic fibrosis, Cell proliferation*

Tropical Journal of Pharmaceutical Research is indexed by Science Citation Index (SciSearch), Scopus, International Pharmaceutical Abstract, Chemical Abstracts, Embase, Index Copernicus, EBSCO, African Index Medicus, JournalSeek, Journal Citation Reports/Science Edition, Directory of Open Access Journals (DOAJ), African Journal Online, Bioline International, Open-J-Gate and Pharmacy Abstracts

INTRODUCTION

Hepatic fibrosis, a disease caused by chronic pathological changes in the liver, often results from the imbalance of liver extracellular matrix metabolism. The incidence of hepatic fibrosis in China is increasing yearly. If the patient is not treated promptly, the condition can worsen, developing into liver cirrhosis, the terminal stage of the progressive hepatic fibrosis, and

subsequently seriously endangering the life and health of the patient [1,2]. The complications of liver cirrhosis are fatal, such as functional liver failure, systemic bacterial infection, and liver cancer. Approximately one million people will die from liver cirrhosis annually worldwide [3,4].

Studies have shown that the activation and proliferation of hepatic stellate cells (HSCs) play vital roles in hepatic fibrosis development [5]. HSCs function as the precursors of myofibroblasts, the presence of which in organs indicates a tissue fibrogenesis status [6].

MicroRNA (miRNA) regulates cell activation, proliferation, and apoptosis [7,8]. Studies have shown that HSC activation and hepatic fibrosis are related to many miRNAs, and differences exist in the correlation between the miRNA levels and hepatic fibrosis in different hepatic fibrosis models [9]. Previous studies have reported that miR-129-5p is under-expressed in liver cancer tissues and cells, and up-regulating its expression can markedly inhibit liver cancer cell proliferation and promote cell apoptosis [10]. In HSCs, Chen *et al* [11] showed that osteopontin (OPN) induces type I collagen expression by regulating the miR-129-5p level. Thus, miR-129-5p may play a crucial role in HSC activation and hepatic fibrosis development. The present study aimed to construct a carbon tetrachloride-induced rat hepatic fibrosis model and explore the effects of miR-129-5p on HSC cell proliferation and migration from *in vitro* assays. The findings may provide a theoretical basis to elucidate the role of miR-129-5p in hepatic fibrosis and rat primary HSC cell biological functions [12].

EXPERIMENTAL

Materials and equipment

Forty 6-week-old, specific pathogen-free male Sprague-Dawley rats were obtained from the Institute of Medical Experimental Animals, Chinese Academy of Medical Sciences and weighed 180 ± 5 g (SCXK; Beijing 2018-0002). The following reagents and equipment were used: Trizol™ Reagent RNA Extraction Kit (Beijing Kangwei Century Co. Ltd); Lipofectamine™ 2000 Transfection Reagent (Invitrogen, USA); Reverse Transcription Kit (TaKaRa, Japan); CCK-8 Kit (Shanghai Biyuntian Biotechnology Co. Ltd); miR-129-5p mimics and negative control (mimics-NC) (Biomics Biotech); fetal bovine serum and DMEM medium (Gibco, USA); rabbit anti-human SGK3 polyclonal antibody, anti-β-catenin polyclonal antibody, anti-α-SMA polyclonal antibody, anti-GAPDH polyclonal antibody, and HRP-labeled goat anti-rabbit IgG (Abcam, USA); real-time fluorescence-based quantitative polymerase chain reaction (RT-qPCR) instrument (BioRad, USA); upright fluorescence microscope (Nikon, Japan); ABI 7500 fluorescence quantitative PCR instrument (ABI, USA); SHELLAB 2406-2 CO_2 incubator (SHELLAB, USA); and CLARIOstar multifunctional microplate reader (BMG LABTECH, Germany).

Ethics approval

All animal experiments were approved by the Research Ethics Committee of Lishui City People's Hospital (Approval no. LLW-FO-403) and were conducted in accordance with the National Institutes of Health Laboratory Animal Care and Use Guidelines [13].

Animal grouping and modeling

Forty SD rats were randomly divided into two groups: control group (n = 20) and model group (n = 20). According to a previous finding [14] and preliminary experiments, CCl_4 induction was used to establish a rat model of hepatic fibrosis: the volume ratio of CCl_4 to olive oil was 2:5. The rats were injected subcutaneously with 0.5 mL/100 g of 40 % CCl_4 oil solution the first time and then with 0.3 mL/100 g of 40 % CCl_4 oil solution twice a week. The control rats were injected with the same dose of 0.9 % sodium chloride solution for 8 weeks. Five rats from each group were anesthetized at the 2^{nd}, 4^{th}, 6^{th}, and 8^{th} weekends using an intraperitoneal injection of sodium pentobarbital (50 mg/kg), and the liver tissues were surgically removed, fixed in 4 % paraformaldehyde, and stored at - 80 °C. All animal experiments were approved by the Laboratory Animal Welfare and Ethics Committee of the Lishui City People's Hospital and were conducted in accordance with the National Institutes of Health Laboratory Animal Care and Use Guidelines [15,16].

Hematoxylin and Eosin (HE) staining

Rat liver tissues were subjected to HE staining. Paraffin sections were prepared routinely; fixed in xylene for 30 min; and dehydrated with 100, 95, 85, and 75 % ethanol for 5 min. After washing with water, the samples were stained with hematoxylin for 10 min, soaked in 1 % hydrochloric acid and then rinsed with water. Next, the sample was stained with eosin solution for 3 min; dehydrated with 75, 85, 95, and 100 % ethanol for 2 min; and then treated with xylene. The slides were then mounted with resin, and the liver tissues were observed under a microscope.

Sirius red staining to evaluate collagen deposition in the liver

Paraffin sections were prepared routinely according to method 2.2, and then the samples were incubated with Sirius red solution at room temperature for 1 h in the dark. After washing and gradient ethanol dehydration, xylene was added, and the slides were mounted with neutral gum and observed under a microscope.

Quantitative real-time polymerase chain reaction (qRT-PCR)

Rat liver tissues were rinsed twice with phosphate-buffered saline (PBS), and the total RNA was extracted according to the manufacturer's instructions for Trizol™ Reagent. Reverse transcription of total RNA into cDNA was performed according to the instructions for the 4 × Reverse Transcription Master Mix Reverse Transcription Kit. Fluorescent quantitative PCR was performed using the SYBR Green qPCR Mix kit and cDNA as a template. The reaction conditions were as follows: initial denaturation at 94 °C for 2 min, followed by 40 cycles of 94 °C for 20 s, and 60 °C for 30 s (Table 1). Using U6 as an internal control, the relative expression of the miR-129-5p gene was determined using the $2^{-\Delta\Delta Ct}$ method.

Isolation and cultivation of rat primary HSCs

Primary HSCs were isolated from healthy rat livers using a two-step enzymatic digestion method [14], followed by classic density gradient centrifugation. Next, the cells were cultured in high-sugar DMEM containing 10 % fetal bovine serum, 2 mmol/L of glutamine, and 1 % streptomycin-penicillin, followed by incubation in a constant temperature cell incubator under 5 % CO_2 at 37 °C for 14 days. The HSCs were collected for follow-up experiments.

Cell transfection

The miR-129-5p mimics, negative control (miR-129-5p NC), and blank control groups were established. After the rat primary HSCs were cultured to the logarithmic growth phase, the cells were digested with trypsin and washed twice. The cells were then adjusted to a density of 3.0×10^6 cells/mL in complete medium, and 200 μL of cell suspension was inoculated into a 6-well plate for 24 h incubation. Next, 5 μL of Lipofectamine™ 2000, 5 μL of Lipofectamine™ 2000 + negative plasmid miR-129-5p NC, or 5 μL of Lipofectamine™ 2000 + 5 μL miR-129-5p mimics was added to an EP tube, incubated at room temperature for 5 min, and mixed with the cells. Serum-free DMEM medium was then added to a final volume of 2 mL. Next, the cells were incubated under 5 % CO_2 at 37 °C with saturated humidity for 6 h. Next, the culture medium was changed to complete medium for further incubation to complete the transfection of rat primary HSCs. After the cells were successfully transfected, qRT-PCR was used to evaluate the intracellular expression of miR-129-5p. HSCs were collected by centrifugation and washed twice with PBS, and total RNA from rat primary HSCs was extracted using Trizol™ Reagent according to the manufacturer's instructions. Reverse transcription of total RNA into total cDNA was performed accordingly, and then fluorescent quantitative PCR was performed using cDNA as a template and following the manufacturer's instructions for the SYBR Green qPCR Mix kit. The reaction conditions were as follows: initial denaturation at 94 °C for 2 min, followed by 40 cycles of 94 °C for 20 s, and 60 °C for 30 s. Using U6 as an internal control, the relative expression of miR-129-5p gene was determined using the $2^{-\Delta\Delta Ct}$ method.

Cell proliferation assay

After transfection, the rat primary HSCs were grown to the logarithmic phase, digested with trypsin, washed twice, and cultured to a density of approximately 3.0×10^3 cells/mL. Each well of a 96-well plate was inoculated with 100 μL of cell suspension. A prepared CCK-8 reagent solution (10 μL of CCK-8 reagent + 90 μL of complete medium) was added to the cell cultures at 24, 48 and 72 h, followed by incubation for 2 h. The cell viability was assessed by A_{450} values using a microplate reader.

Transwell assay

After 48 h of transfection, the primary rat HSCs were digested and the cell concentration was adjusted to a density of 3×10^5 cells/mL using serum-free DMEM medium.

Table 1: Primers used in this study

Gene	Forward primer	Reverse primer
miR-129-5p	5'-GCGGCTTTTTGCGGTCTGG-3'	5'-GTGCAGGGTCCGAGGT-3'
U6	5'-GCTCGCTTCGGCAGCACA-3'	5'-AACGCTTCACGAATTTGCGT-3'

Next, the cells were inoculated into the Transwell chamber, and 600 µL of serum-containing culture medium was added to the lower chamber. The Transwell chamber was placed in an incubator for routine incubation and removed after 48 h. Next, the cells were fixed for 30 min, followed by staining with crystal violet. The upper layer of cells was wiped off with a cotton swab. These cells were then observed under a microscope and photographed, and the invasive cells were counted.

Western blot analysis

After transfection, the rat primary HSCs were grown to the logarithmic phase. The cells of each group were collected by centrifugation, and total protein was extracted using lysis buffer. The total protein concentration was determined using the bicinchoninic acid protein quantification kit, and equal amounts of protein were subjected to 12 % sodium dodecyl sulfate–polyacrylamide gel electrophoresis, followed by protein transfer to polyvinylidene fluoride membranes. The membranes were blotted with 5 % skimmed milk and then were incubated with anti-GAPDH (1:10,000), anti-SGK3 (1:1,000), anti-β-catenin (1:1,000), or anti-α-SMA (1:1,000) primary antibodies overnight. The membranes were washed three times with wash buffer and then were incubated with horseradish peroxidase (HRP)-labeled goat anti-rabbit IgG (1:10,000) for 2 h. After washing the membranes three times with wash buffer, the protein signals on the membranes were visualized using an enhanced chemiluminescence system. The expression of proteins was evaluated by the density of protein bands using ImageJ.

Dual luciferase assay

The constructed luciferase reporter plasmids (WT-SGK3 and MT-SGK3) were co-transfected into rat primary HSCs with miR-129-5p NC and miR-129-5p mimics (final concentration: 50 nM), respectively. The cells were incubated for 48 h after which a dual luciferase reporter gene detection system was used to assess luciferase activity.

Statistical analysis

SPSS 17.0 software was used to statistically analyze the data. The data were expressed as means ± standard deviation ($\bar{x}$ ± s). One-way analysis of variance was used for comparison between groups, and the SNK-q test was used for pairwise comparisons. $p < 0.05$ indicated a statistically significant difference.

RESULTS

Changes in miR-129-5p expression during hepatic fibrosis

The liver tissues of the model and control groups were subjected to HE and Sirius red staining. HE staining revealed that the liver tissues in the control group exhibited integrated cell morphology with cells neatly arranged in a radial pattern and no inflammatory cell infiltration, degeneration, necrosis, or fibrotic hyperplasia. In the model group, small fibrotic nodules, inflammation, balloon degeneration, and necrosis appeared at each time point, and the hepatic fibrosis status gradually worsened over time (Figure 1 A, upper panels). Sirius red staining revealed no collagen deposition in the hepatic portal vein and portal areas in the control group. In the model group, a large amount of collagen deposition was observed in the hepatic portal vein and portal areas, and the situation became more severe over time (Figure 1 A, bottom panels). RT-qPCR showed that the miR-129-5p expression level gradually decreased during CCl_4-induced hepatic fibrosis in rats, and the difference in expression was statistically significant ($p < 0.05$; Figure 1 B).

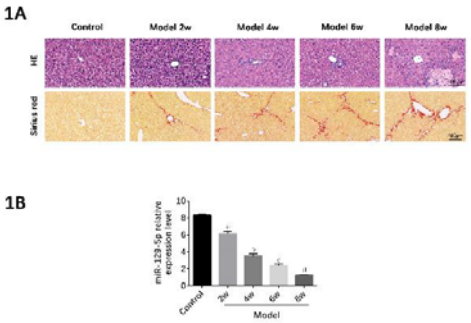

Figure 1: (A) Morphological changes in liver tissues of the model and control groups as demonstrated by HE and Sirius red staining. (B) Relative expression level of miR-129-5p in the model and control groups during hepatic fibrosis. Different letters on the bar graph of the model group indicate significant differences in gene expression compared with the control group ($p < 0.05$)

Effect of miR-129-5p overexpression on the cell proliferation ability of rat primary HSCs

After transfection, the expression level of miR-129-5p in the rat primary HSCs in the miR-129-5p mimics group (2.45 ± 0.21) was significantly increased compared with that in the miR-129-5p NC group (0.96 ± 0.01) and blank control group (1.00 ± 0.04) ($F = 243.30$; $p < 0.001$; Figure 2). Additionally, the CCK-8 assay showed that the cell proliferation rates of rat primary HSCs in the

miR-129-5p mimics group at 24 h, 48 h, and 72 h, were significantly lower than those in the miR-129-5p NC and blank control groups ($p < 0.05$).

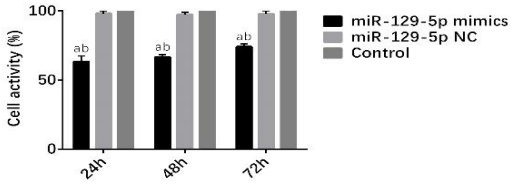

Figure 2: Expression of miR-129-5p and cell proliferation in rat primary HSCs after transfection. *a* represents the comparison with the miR-129-5p NC group, $p < 0.05$; *b* represents the comparison with the blank control group, $p < 0.05$

Effect of miR-129-5p overexpression on the cell migration potential of rat primary HSCs

After 48 h of transfection, the cell migration potential of rat primary HSCs in the miR-129-5p mimics group was decreased significantly compared with that in the miR-129-5p NC and blank control groups ($p < 0.05$; Figure 3). This result suggests that miR-129-5p inhibits the cell migration of rat primary HSCs.

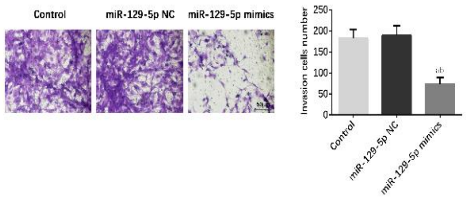

Figure 3: Effect of miR-129-5p on the cell migration potential of rat primary HSCs. *a* represents the comparison with the miR-129-5p NC group, $p < 0.05$; *b* represents the comparison with the blank control group, $p < 0.05$

MiR-129-5p targets serum- and glucocorticoid-regulated kinase 3 (SGK3)

Using the target gene prediction website Targetscan, miR-129-5p was predicted to have binding sites on SGK3. The dual luciferase reporter gene assay revealed (Figure 4) that miR-129-5p mimics significantly inhibited WT-SGK3 3´UTR luciferase activity ($p < 0.05$) but demonstrated no effect on the MT-SGK3 3´UTR luciferase activity ($p > 0.05$).

Effect of miR-129-5p overexpression on SGK3, β-catenin, and α-smooth muscle actin (α-SMA) protein expression in rat primary HSCs

Western blotting analysis demonstrated that the protein expression levels of SGK3, β-catenin, and α-SMA were significantly decreased in cells transfected with miR-129-5p mimics compared with the miR-129-5p NC and blank control groups ($p < 0.05$; Figure 5).

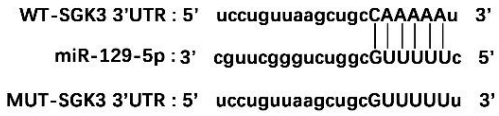

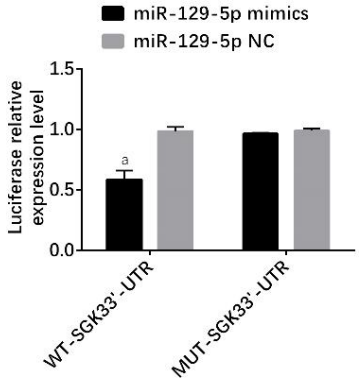

Figure 4: Target relationship between miR-129-5p and SGK3. *a* represents the comparison with the miR-129-5p NC group, $p < 0.05$

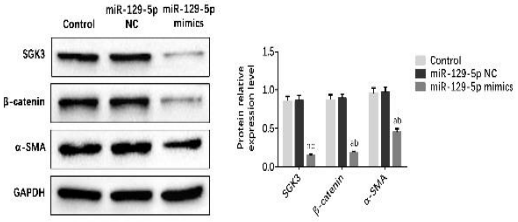

Figure 5: Effect of miR-129-5p overexpression on SGK3, β-catenin, and α-SMA protein expression in rat primary HSCs. *a* represents the comparison with the miR-129-5p NC group, $p < 0.05$; *b* represents the comparison with the blank control group, $p < 0.05$

DISCUSSION

Hepatic fibrosis is a common disease with a high incidence in China, and its main pathological mechanism is the excessive deposition of extracellular matrix and fibrotic scar formation [17]. Hepatic fibrosis is caused by diseases such as non-alcoholic steatohepatitis, alcoholic liver disease, viral hepatitis, and parasitic infections [18]. HSC activation is essential to the development of hepatic fibrosis[19]. Therefore, the formation mechanism of hepatic fibrosis and activation mechanism of HSCs warrant further investigation.

MiR-129-5p is a tumor suppressor that inhibits tumor development by targeting multiple oncogenes in liver cancer [20, 21]. Based on previous studies, the present study replicated the CCl_4-induced rat hepatic fibrosis model and investigated for the first time the effect of miR-129-5p on hepatic fibrosis. HE staining and Sirius red staining results showed that the degree of hepatic fibrosis in the rat liver tissues of the model group gradually increased over time. Additionally, miR-129-5p expression gradually decreased during CCl_4-induced hepatic fibrosis, demonstrating that miR-129-5p expression in hepatic fibrosis was inhibited. Based on the above-mentioned results, the relationship between miR-129-5p and cell proliferation and migration of rat primary HSCs was investigated. After transfection with the miR-129-5p gene, the proliferation rate and migration ability of rat primary HSCs were significantly reduced, suggesting that the low expression level of miR-129-5p during CCl_4-induced rat hepatic fibrosis promotes HSC activation, but the detailed molecular mechanism warrants further study.

Typically, HSCs are in a static state, but they are rapidly activated when the liver is stimulated, producing many fibroblasts, promoting the synthesis and inhibiting the degradation of extracellular matrix (ECM), and causing excessive deposition of ECM in the liver. The effect of miRNAs on the biological functions of HSCs is achieved by regulating their corresponding target genes [18,19]. Concerning the role of miR-129-5p in hepatic fibrosis, miR-129-5p overexpression in HSCs was reported to inhibit the induction of type I collagen synthesis [11]. However, no study has identified SGK3 as a target gene of miR-129-5p. In the present study, SGK3 was identified as a new target of miR-129-5p. SGK3 belongs to the AGC protein kinase family and has extremely high homology with the catalytic domain of AKT1. As a downstream target gene of PI3K, SGK3 participates in many crucial human physiological processes, such as cell growth, proliferation, survival, and migration, and SGK3 gene silencing inhibits MB-474 cell proliferation and promotes its apoptosis [22].

In the present study, following the up-regulation of miR-129-5p expression, significantly decreased expression was observed not only in SGK3 but also in β-catenin and α-smooth muscle actin (α-SMA), which is only expressed in HSCs in liver tissues and is considered a marker of HSC activation and proliferation. Studies have highlighted that abnormal activation of the Wnt/β-catenin signaling pathway and subsequent HSC activation are critical causes of hepatic fibrosis. β-Catenin is the key factor to promote fibrosis, and its high expression promotes collagen fiber formation, α-SMA synthesis and secretion, and HSC activation [23]. In addition, Kong *et al* [24] showed that inhibiting SGK3 down-regulates β-catenin expression through the proteasome pathway. Therefore, miR-129-5p may participate in HSC activation through targeted regulation of SGK3 to down-regulate β-catenin expression.

CONCLUSION

MiR-129-5p is expected to become a specific miRNA to treat hepatic fibrosis. Hepatic fibrosis reduces the expression level of miR-129-5p, laying the foundation for the clinical diagnosis and treatment of hepatic fibrosis; however, the related mechanism requires further investigation.

DECLARATIONS

Conflict of Interest

No conflict of interest associated with this work.

Contribution of Authors

We declare that this work was performed by the authors named in this article and all liabilities pertaining to claims relating to the content of this article will be borne by the authors. Chen Li designed the study and supervised the data collection. Yaohong Xu analyzed and interpreted the data. Xiaofu Lin prepared the manuscript for publication and reviewed the draft of the manuscript. All the authors have read and approved the manuscript.

Open Access

REFERENCES

1. *Wu S, Liu L, Yang S, Kuang G, Gong XJI, Immunotoxicology. Paeonol alleviates CCl_4-induced liver fibrosis through suppression of hepatic stellate cells activation via inhibiting the TGF-β/Smad3 signaling. Immunopharmacol Immunotoxicol 2019; 41(3): 1-8.*

2. Hu ZW, Wang WXJTJoPR. Effect of Carthamus tinctorius L Extract on Diethylnitrosamine-Induced Liver Cirrhosis in Rats. Trop J Pharm Res 2015; 14(7): 1213-1216.
3. Global burden of stroke and risk factors in 188 countries, during 1990-2013: a systematic analysis for the Global Burden of Disease Study 2013. Lancet Neurol. 2016; 15(9): 913-924.
4. Tsochatzis EA, Bosch J, Burroughs AKJL. Liver cirrhosis. The Lancet, 2014, 383(9930): 1749-1761.
5. Zhu J, Zhang Z, Zhang Y, Li W, Zheng W, Yu J, Wang B, Chen L, Zhuo Q, Chen LJBBRC. MicroRNA-212 activates hepatic stellate cells and promotes liver fibrosis via targeting SMAD7. Biochem Biophys Res Commun 2018; 496(1): 176-183.
6. Higashi T, Friedman SL, Hoshida YJADDR. Hepatic stellate cells as key target in liver fibrosis. Adv Drug Deliv Rev 2017; 121:27-42.
7. Andrea N, Monika K, Natalia E, Jia H, Margarete OJFiP. microRNA are Central Players in Anti- and Profibrotic Gene Regulation during Liver Fibrosis. Front Physiol 2012; 3(3): 49.
8. Brennecke J, Hipfner DR, Stark A, Russell RB, Cohen SMJC. bantam Encodes a Developmentally Regulated microRNA that Controls Cell Proliferation and Regulates the Proapoptotic Gene hid in Drosophila. Cell 2003; 113(1): 25-36.
9. Xin XJFiB. MicroRNA in hepatic fibrosis and cirrhosis. Front Biosci 2014; 19(8): 1418-1424.
10. Li Z, Lu J, Zeng G, Pang J, Zhang JJCD, Disease. MiR-129-5p inhibits liver cancer growth by targeting calcium calmodulin-dependent protein kinase IV (CAMK4). Cell Death Dis 2019;10(11):789.
11. Chen Y, Ou Y, Dong J, Yang G, Zeng Z, Liu Y, Liu B, Li W, He X, Lan TJECR. Osteopontin promotes collagen I synthesis in hepatic stellate cells by miRNA-129-5p inhibition. Exp Cell Res 2018; 362(2): 343-348.
12. Karunakaran K, Navaneethan G, Elango K. Development and validation of a stability-indicating RP-HPLC method for simultaneous determination of paracetamol, tramadol HCl and domperidone in a combined dosage form. Trop J Pharm Res 2012; 11(1): 99-106.
13. Health NIo. Guide for the care and use of laboratory animals: National Academies; 1985.
14. Zeng C, Wang YL, Xie C, Sang Y, Zhuang SMJO. Identification of a novel TGF-β-miR-122-fibronectin 1/serum response factor signaling cascade and its implication in hepatic fibrogenesis. Oncotarget 2015; 6(14): 12224-12233.
15. Council NR. Guide for the care and use of laboratory animals: National Academies Press; 2010.
16. Helsinki WJHCT. World Medical Association Declaration of Helsinki: Ethical Principles for Medical Research Involving Human Subjects. JAMA 2000; 2(4): 92-95.
17. Bellan M, Castello LM, Pirisi MJJoC, Hepatology T. Candidate Biomarkers of Liver Fibrosis: A Concise, Pathophysiology-oriented Review. J Clin Transl Hepatol 2018; 6(3): 1-9.
18. Wallace M, Friedman S, Mann DJSiLD. Emerging and disease-specific mechanisms of hepatic stellate cell activation. Semin Liver Dis 2015; 35(02): 107-118.
19. Zhang XW, Zhou JC, Peng D, Hua F, Hu ZWJA. Disrupting the TRIB3-SQSTM1 interaction reduces liver fibrosis by restoring autophagy and suppressing exosome-mediated HSC activation. Autophagy 2019; 16(5): 1-14.
20. Shaker OG, Abdelwahed MY, Ahmed NA, Hassan EA, Ahmed TI, Abousarie MA, Ayoub SEJIL. Evaluation of serum long noncoding RNA NEAT and MiR-129-5p in hepatocellular carcinoma. IUBMB Life 2019; 71(10): 1571-1578.
21. Zhang D, Cao J, Zhong Q, Zeng L, Liu FJB, Biomedecine p, pharmacotherapie. Long noncoding RNA PCAT-1 promotes invasion and metastasis via the miR-129-5p-HMGB1 signaling pathway in hepatocellular carcinoma. Biomed Pharmacother 2017; 95: 1187-1193.
22. Hannan R, Bruhn, Pearson R, Management SJC, Research. AKT-independent PI3-K signaling in cancer – emerging role for SGK3. Cancer Manag Res. 2013; 5: 281-292.
23. Xiaoli, Rong, Junzhi, Liu, Xia, Yao, Tiechao, Jiang, Yimin, Research WJSC, et al. Human bone marrow mesenchymal stem cells-derived exosomes alleviate liver fibrosis through the Wnt/β-catenin pathway. Stem Cell Res Ther 2019; 10(1): 98.
24. Xin, Kong, Fengchao, Liu, Jian, Oncotarget GJ. MiR-155 promotes epithelial-mesenchymal transition in hepatocellular carcinoma cells through the activation of PI3K/SGK3/β-catenin signaling pathways. Oncotarget 2016; 7(40): 66051-66060.